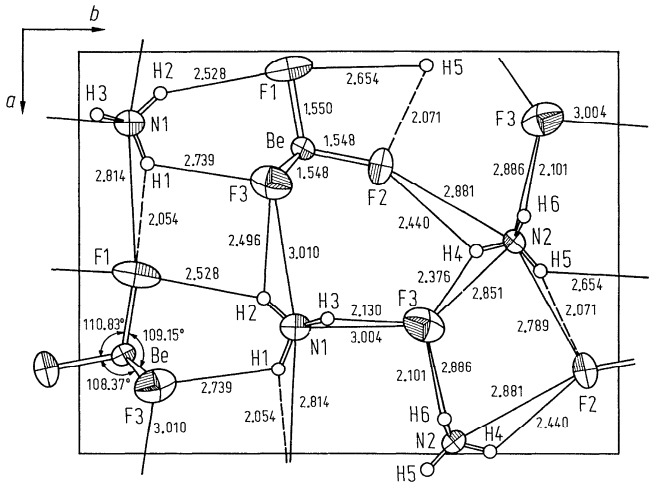

Fig. 39A-3-001. $(NH_4)_2BeF_4$. Structure of phase I [79Ono]. Projection on (001). Interatomic distances [Å] and bond angles [°] in the figure are obtained at 20(1) °C. Dashed lines indicate proposed hydrogen bonds.

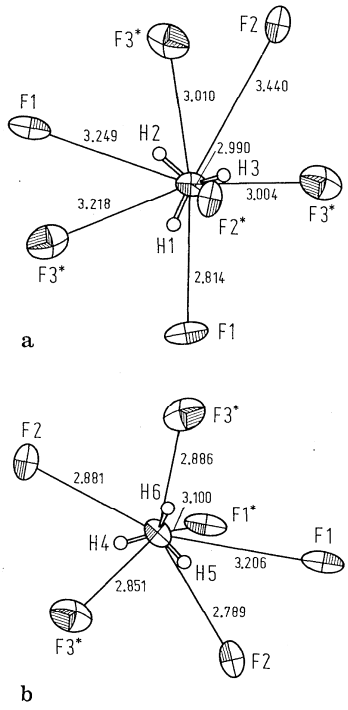

Fig. 39A-3-002. $(NH_4)_2BeF_4$. Structure of phase I [79Ono]. Environments of ammonium ions viewed along the *c* axis; (**a**) around $N(1)H_4$, (**b**) around $N(2)H_4$. The atoms labeled by "*" are above and below the mirror plane. Interatomic distances [Å].

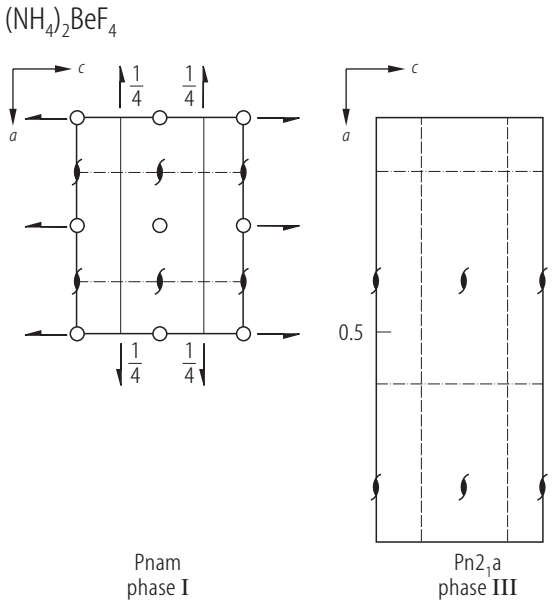

Fig. 39A-3-003. $(NH_4)_2BeF_4$. Structure [79Ono]. Unit cell relation between phase I and phase III. Solid line: mirror plane, dashed line: axial glide plane, dashed-dotted line: diagonal glide plane.

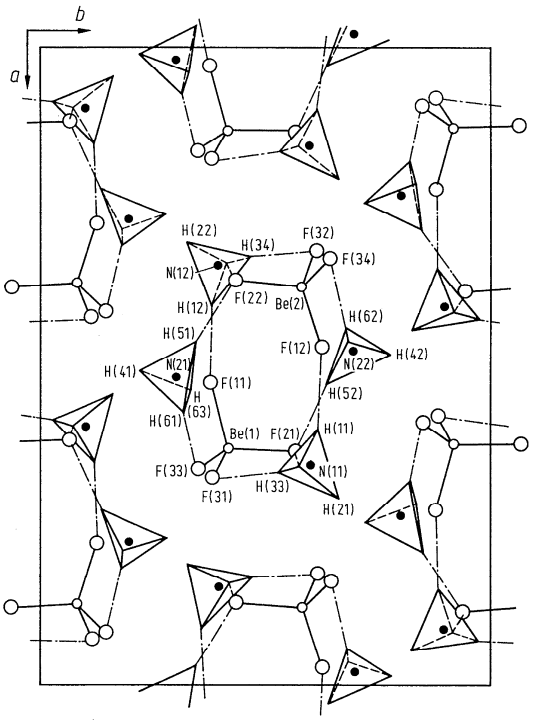

Fig. 39A-3-004. $(NH_4)_2BeF_4$. Structure of phase III [79Ono]. Projection on (001). Ammonium ions are shown by tetrahedra, where hydrogen atoms occupy the corners. The proposed hydrogen bonds are indicated by dashed-dotted lines.

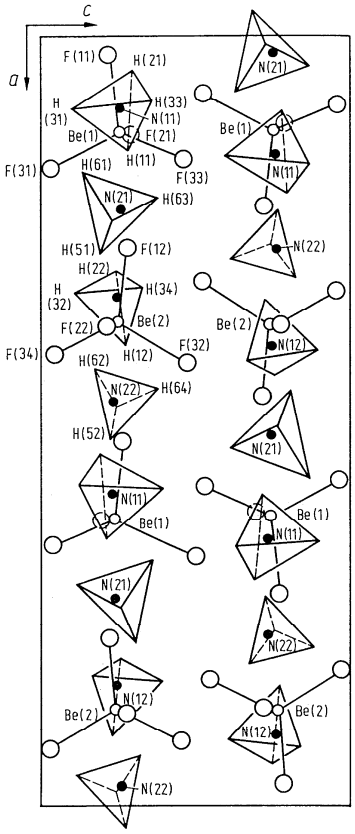

Fig. 39A-3-005. $(NH_4)_2BeF_4$. Structure of phase III [79Ono]. Projection on (010).

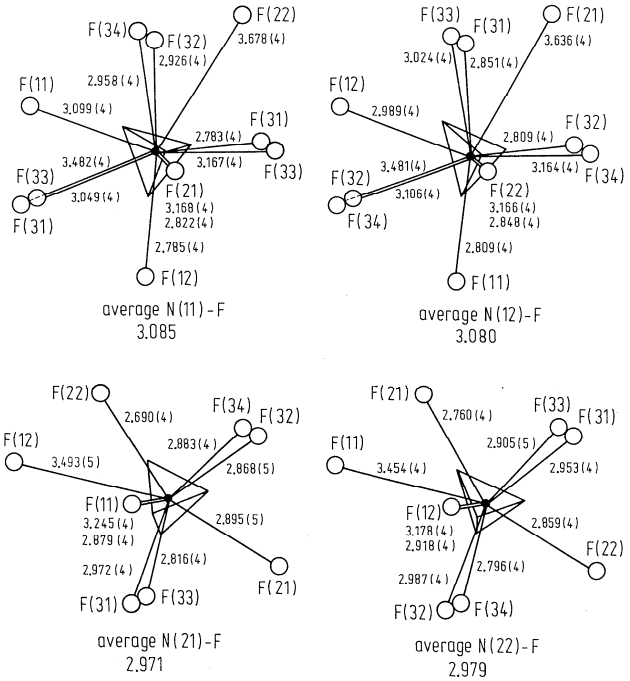

Fig. 39A-3-006. $(NH_4)_2BeF_4$. Structure of phase III [79Ono]. Environments of the ammonium ions viewed along the *c* axis. Numerals are interatomic distances [Å] at $T = -140$ °C.

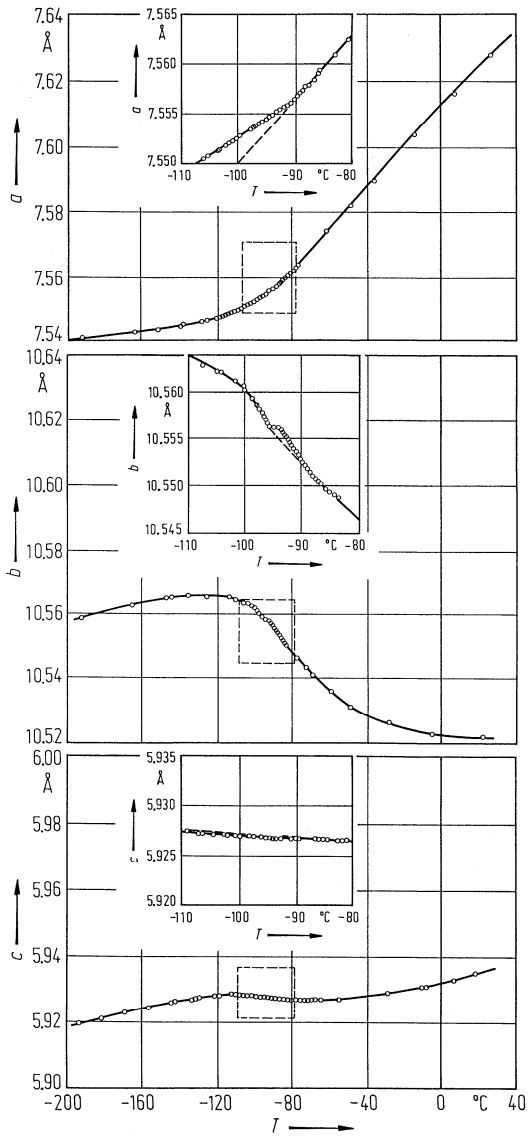

Fig. 39A-3-007. $(NH_4)_2BeF_4$. *a*, *b*, *c* vs. *T* [81Ues]. *a*, *b*, *c*: basic unit cell parameters.

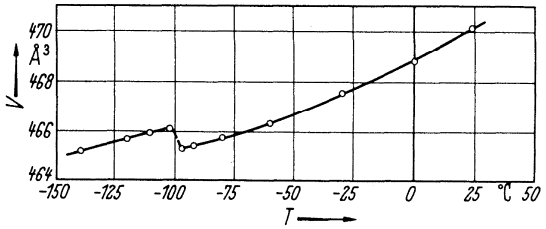

Fig. 39A-3-008. $(NH_4)_2BeF_4$. *V* vs. *T* [58Hos]. *V*: basic unit cell volume.

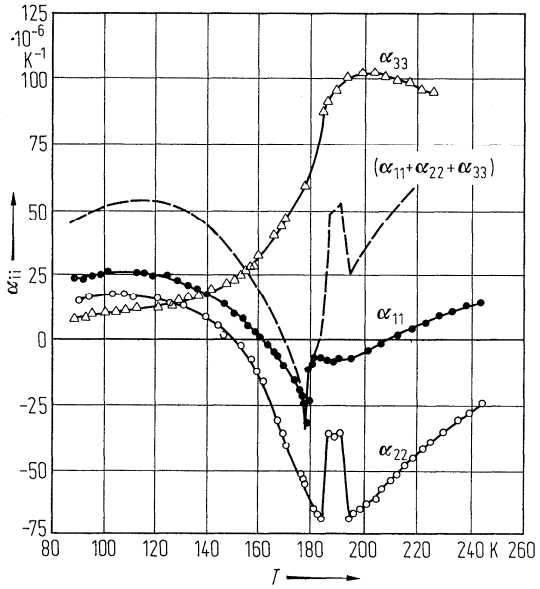

Fig. 39A-3-009. $(NH_4)_2BeF_4$. α_{ii} vs. T [74Zhd]. α_{11}, α_{22}, α_{33}: linear thermal expansion coefficients along the a, b, c axes.

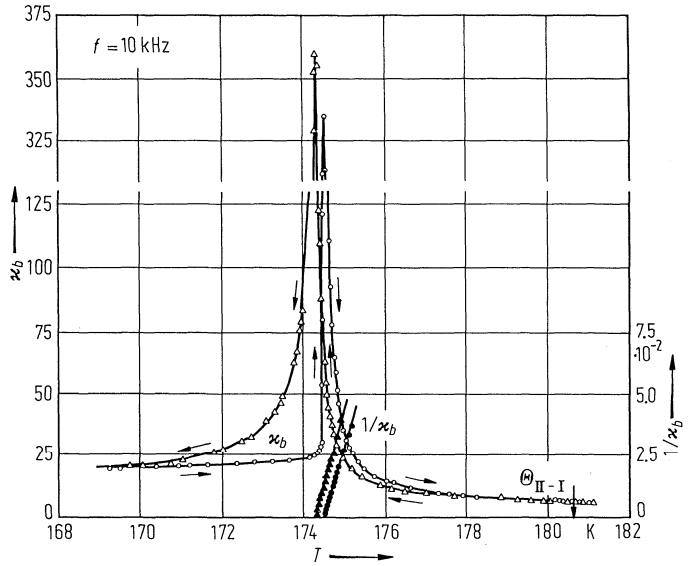

Fig. 39A-3-010. $(NH_4)_2BeF_4$. κ_b, $1/\kappa_b$ vs. T [82Str]. f = 10 kHz.

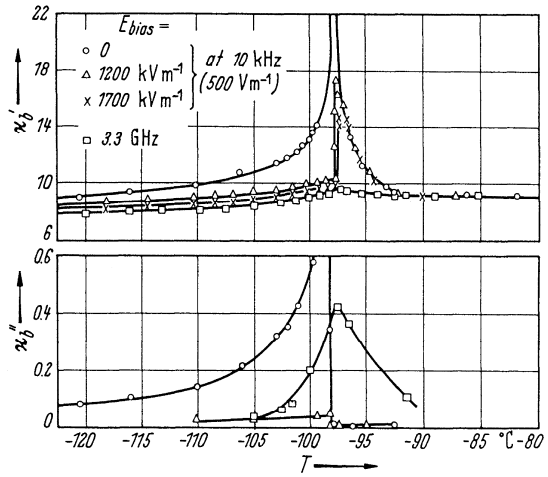

Fig. 39A-3-011. $(NH_4)_2BeF_4$. κ_b', κ_b'' vs. T [66Ohs].

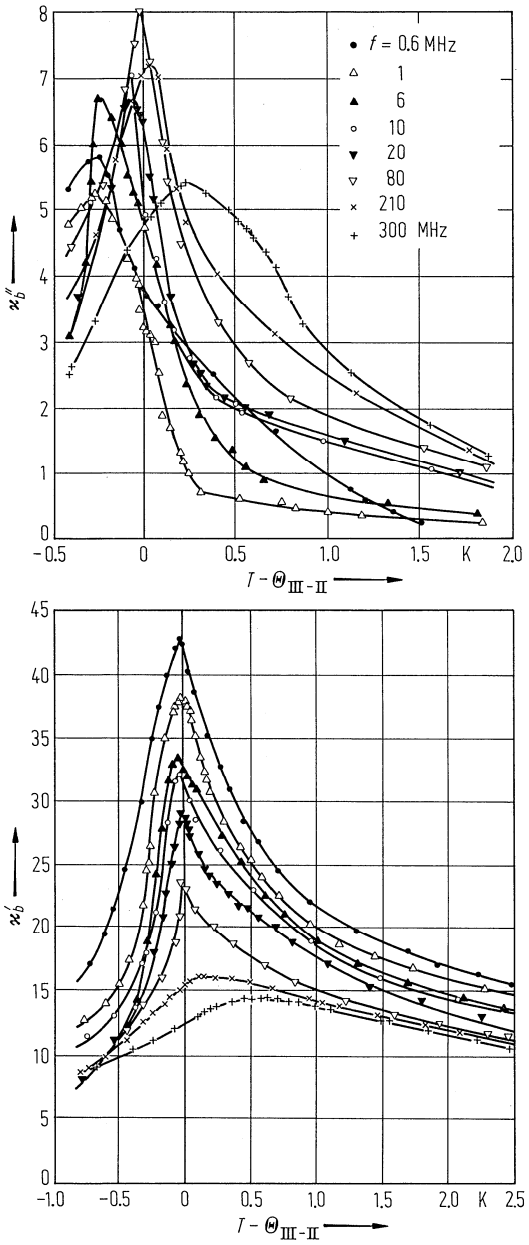

Fig. 39A-3-012. $(NH_4)_2BeF_4$. κ_b', κ_b'' vs. $T - \Theta_{III-II}$ [84Jak]. Parameter: *f*.

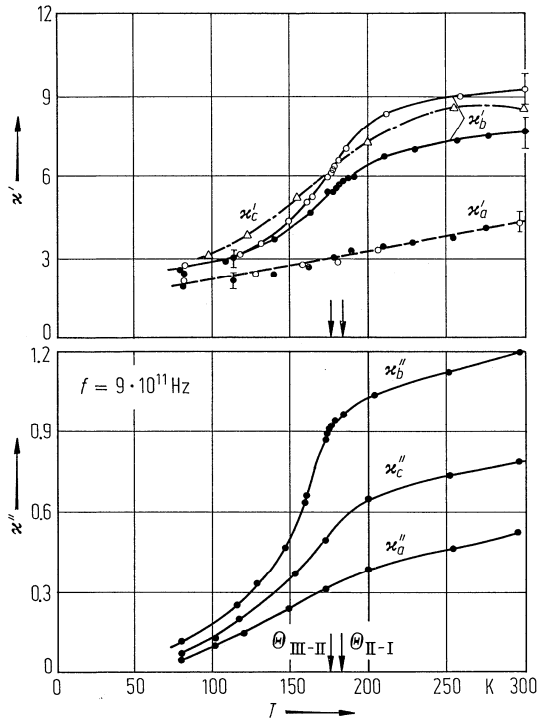

Fig. 39A-3-013. $(NH_4)_2BeF_4$. κ', κ'' vs. T [80Pet]. Parameter: f. Open circle: $f = 1.95 \cdot 10^{11}$ Hz, open triangle: $4.2 \cdot 10^{11}$ Hz, full circle: $9.0 \cdot 10^{11}$ Hz.

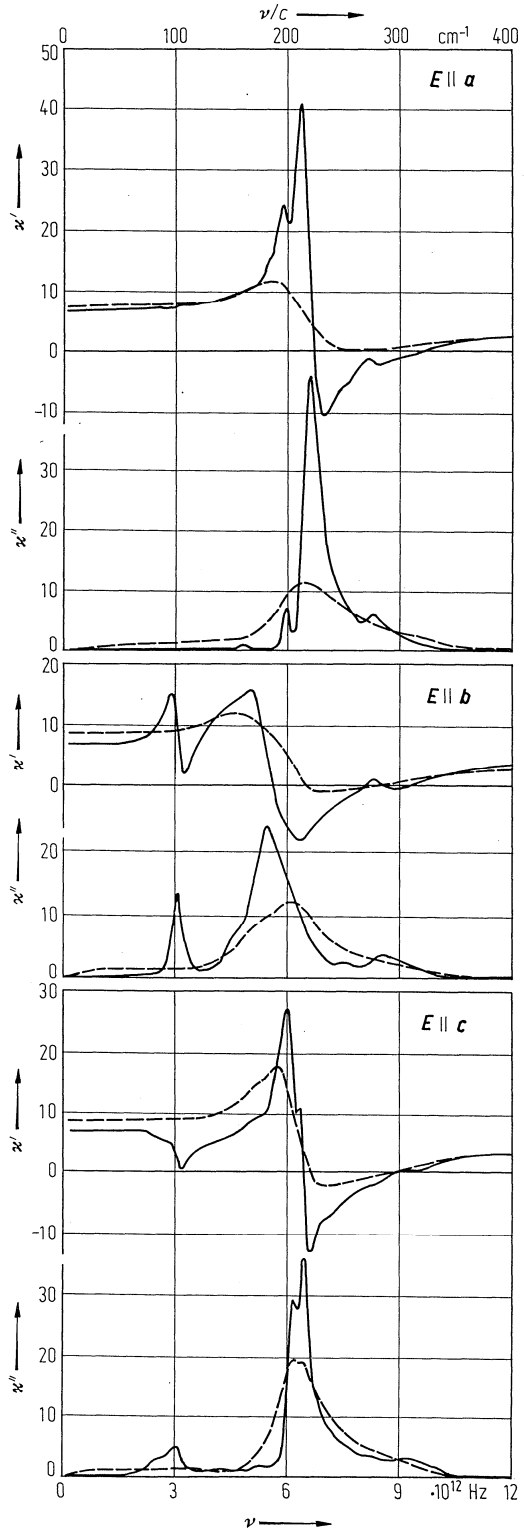

Fig. 39A-3-014. $(NH_4)_2BeF_4$. κ', κ'' vs. ν [80Pet]. Parameter: *T*. Full curves: at 90 K, broken curves: at 300 K. The part below $1.02 \cdot 10^{12}$ Hz is calculated from transmission measurements, the part above $1.02 \cdot 10^{12}$ Hz is calculated by Kramers-Kronig analysis of reflectivity data.

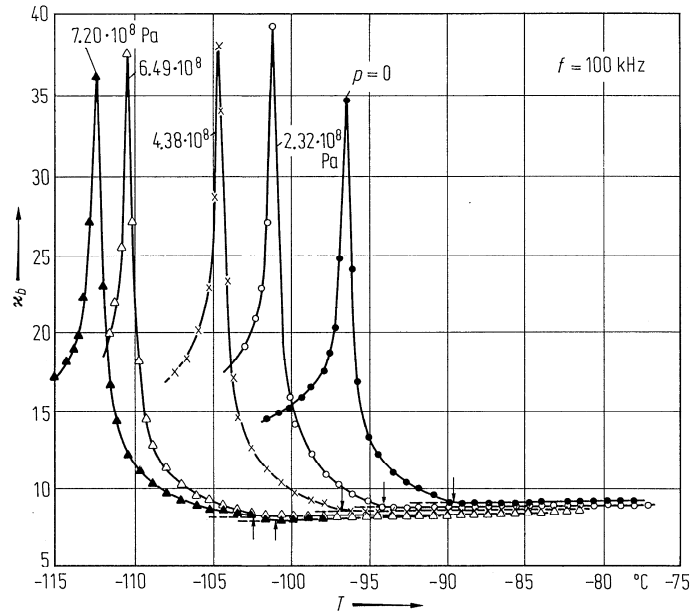

Fig. 39A-3-015. $(NH_4)_2BeF_4$. κ_b vs. T [74Ges]. Parameter: p. The vertical arrow on each curve shows the break at Θ_{II-I}.

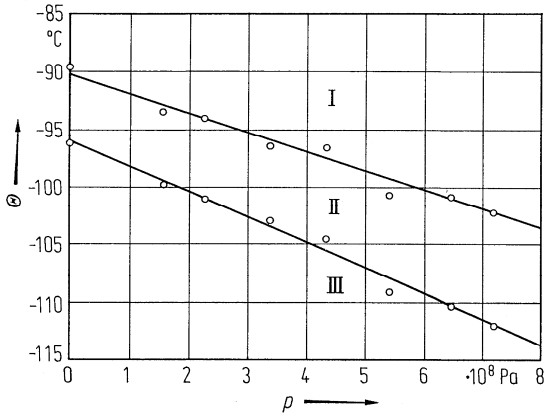

Fig. 39A-3-016. $(NH_4)_2BeF_4$. Θ vs. p [74Ges].

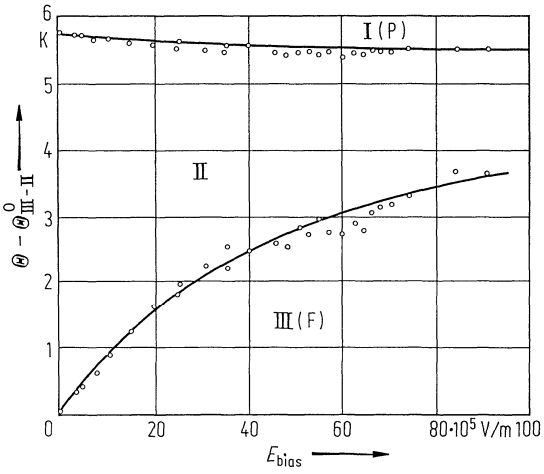

Fig. 39A-3-017. $(NH_4)_2BeF_4$. $\Theta - \Theta^0_{III-II}$ vs. E_{bias} [84Lev]. Θ^0_{III-II} : Θ_{III-II} at $E_{bias} = 0$.

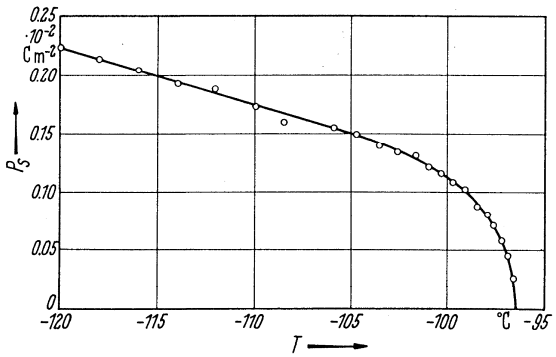

Fig. 39A-3-018. $(NH_4)_2BeF_4$. P_s vs. T [58Hos].

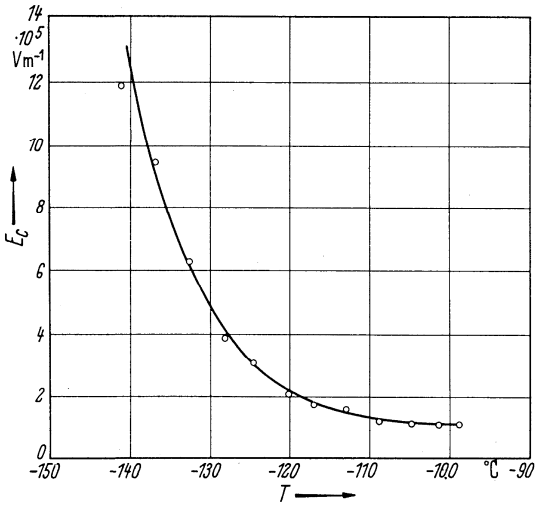

Fig. 39A-3-019. $(NH_4)_2BeF_4$. E_c vs. T [58Hos].

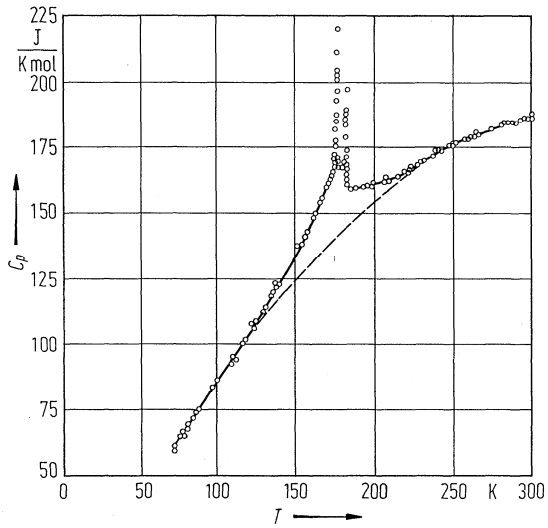

Fig. 39A-3-020. $(NH_4)_2BeF_4$. C_p vs. T [83Str]. C_p: molar heat capacity at constant pressure.

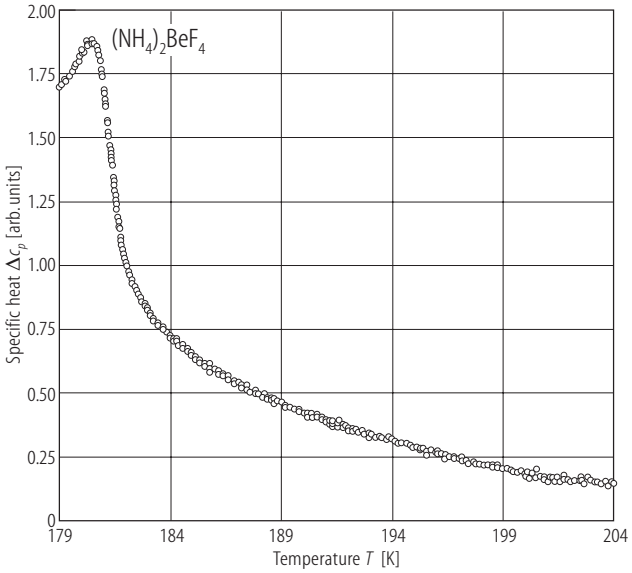

Fig. 39A-3-021. $(NH_4)_2BeF_4$. Δc_p vs. T [93Hag]. Δc_p: anomalous part of specific heat at constant pressure. ac calorimetric measurement.

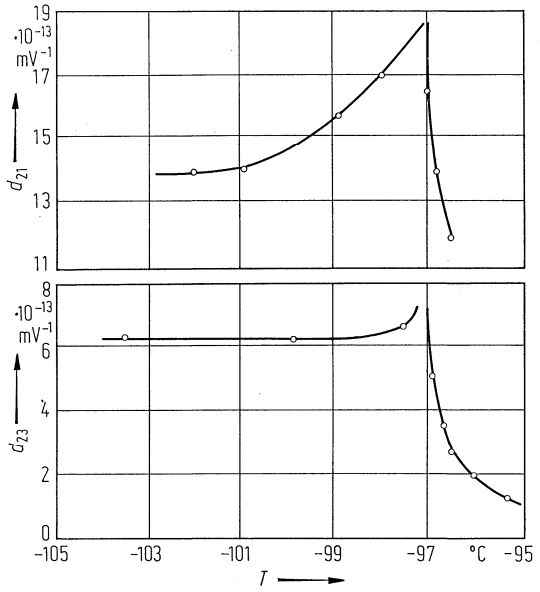

Fig. 39A-3-022. $(NH_4)_2BeF_4$. d_{21}, d_{23} vs. T [79Sor].

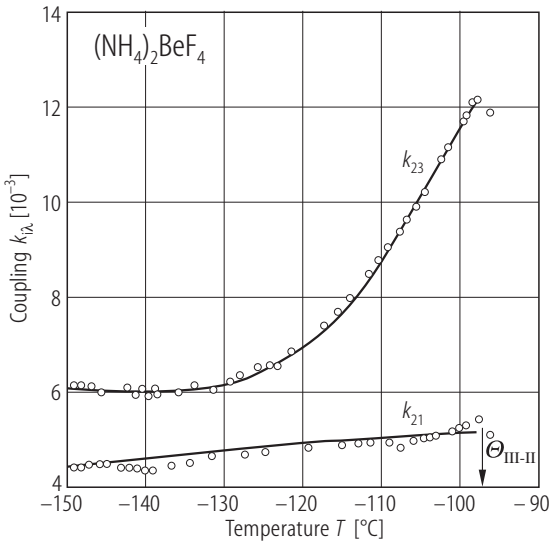

Fig. 39A-3-023. $(NH_4)_2BeF_4$. $k_{i\lambda}$ vs. T [89Sas]. $k_{i\lambda}$: electromechanical coupling coefficient measured by composite-bar resonator method.

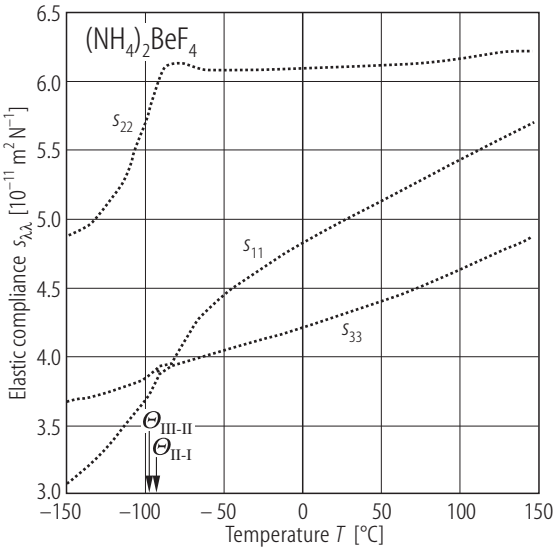

Fig. 39A-3-024. $(NH_4)_2BeF_4$. $s_{\lambda\lambda}$ vs. T [89Sas]. $s_{\lambda\lambda}$: elastic compliance measured by composite-bar resonator method.

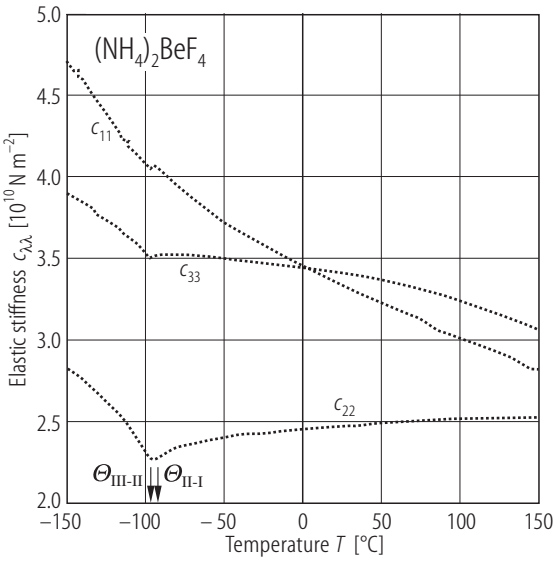

Fig. 39A-3-025. $(NH_4)_2BeF_4$. $c_{\lambda\lambda}$ vs. T [89Sas]. $c_{\lambda\lambda}$: elastic stiffness measured by pulse-echo overlap method at 15 MHz.

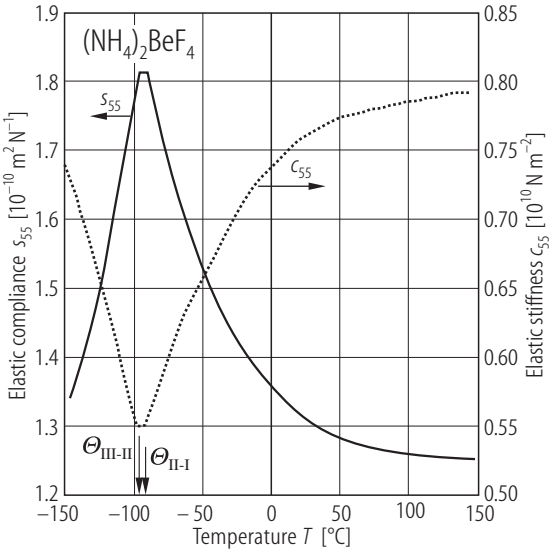

Fig. 39A-3-026. $(NH_4)_2BeF_4$. s_{55}, c_{55} vs. T [89Sas].

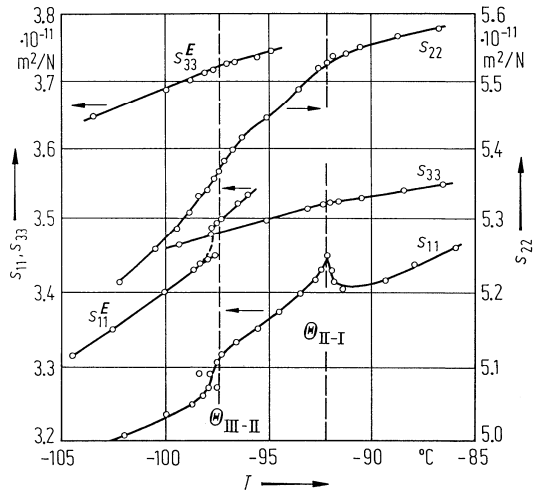

Fig. 39A-3-027. $(NH_4)_2BeF_4$. $s_{\lambda\lambda}$ vs. T [79Sor].

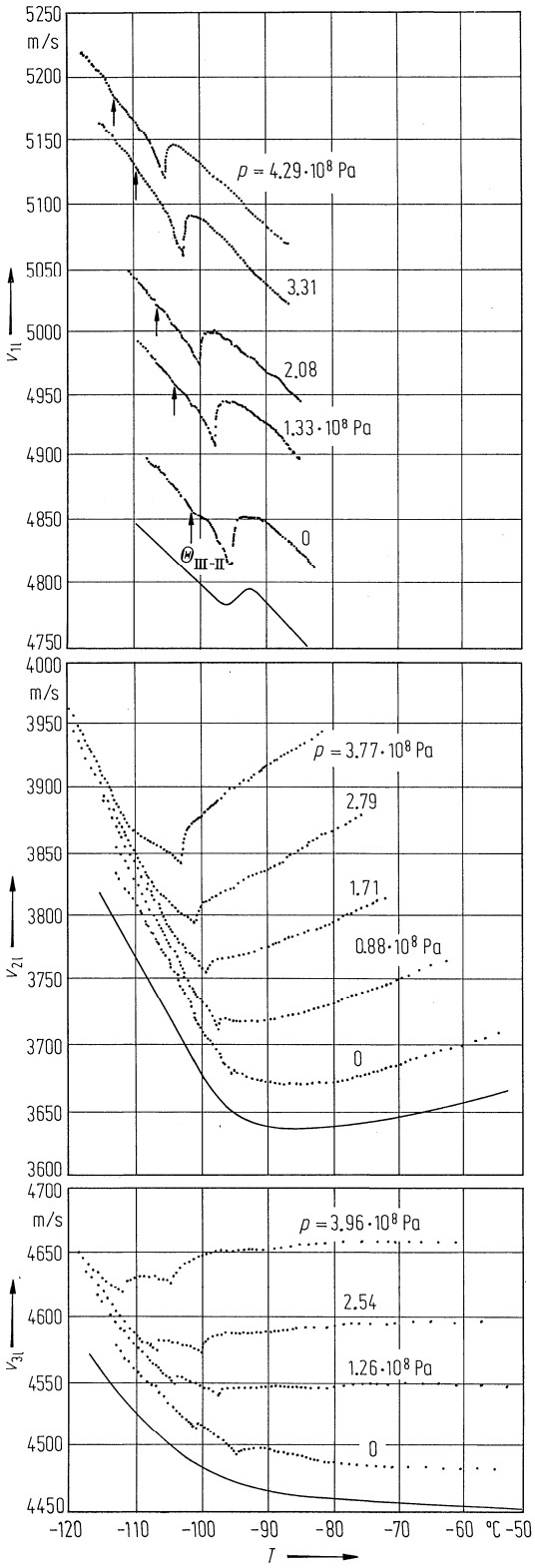

Fig. 39A-3-028. $(NH_4)_2BeF_4$. v_{il} vs. T [82Hik]. Parameter: p. v_{il}: longitudinal sound velocity in x_i-direction. Solid lines indicate the results of Brillouin scattering measurement.

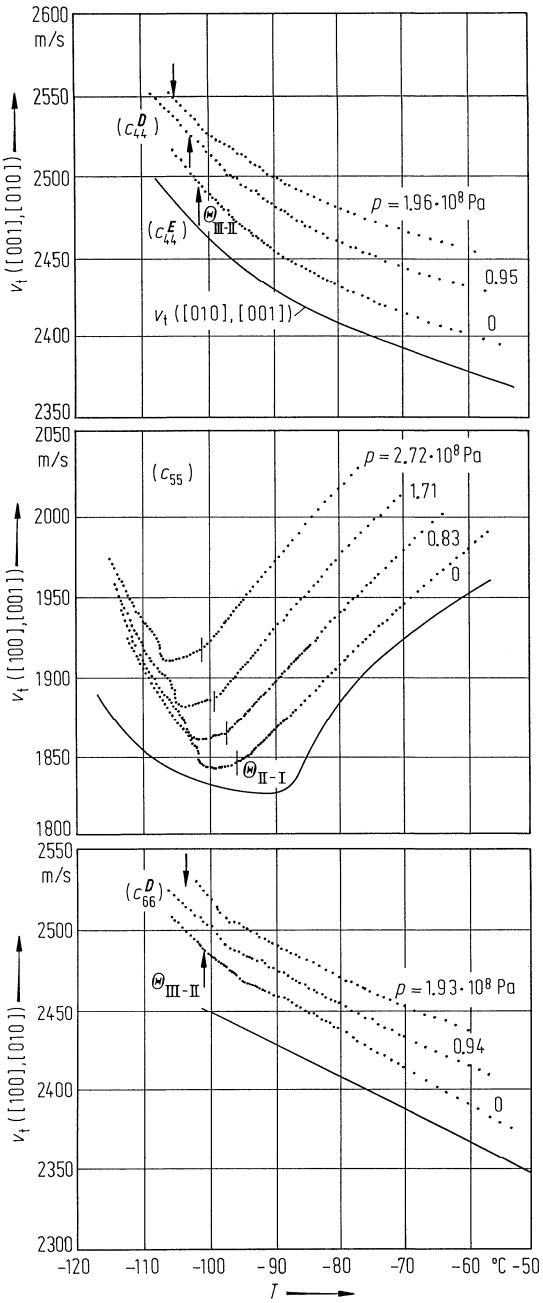

Fig. 39A-3-029. $(NH_4)_2BeF_4$. $v_t(\boldsymbol{k}, \boldsymbol{u})$ vs. T [82Hik]. Parameter: p. $v_t(\boldsymbol{k}, \boldsymbol{u})$: transverse sound velocity with wave vector $\boldsymbol{k}$ and polarization $\boldsymbol{u}$. Elastic constants in parentheses indicate the corresponding elastic constants below Θ_{III-II}. Solid lines indicate the results of Brillouin scattering measurement.

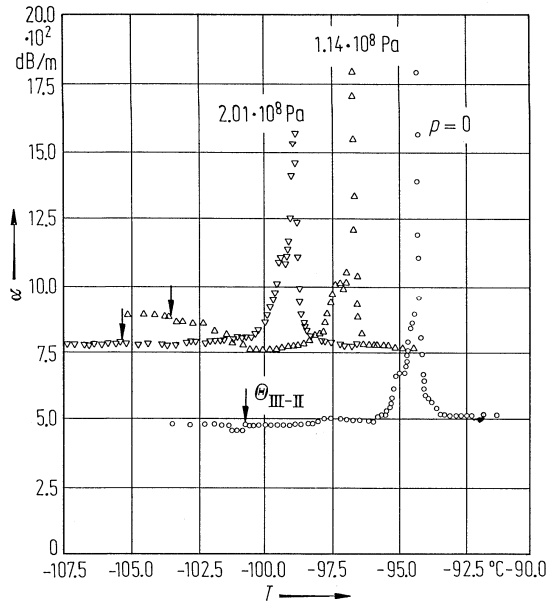

Fig. 39A-3-030. $(NH_4)_2BeF_4$. α vs. T [82Hik]. Parameter: p. α: attenuation of longitudinal sound propagated along [100] direction.

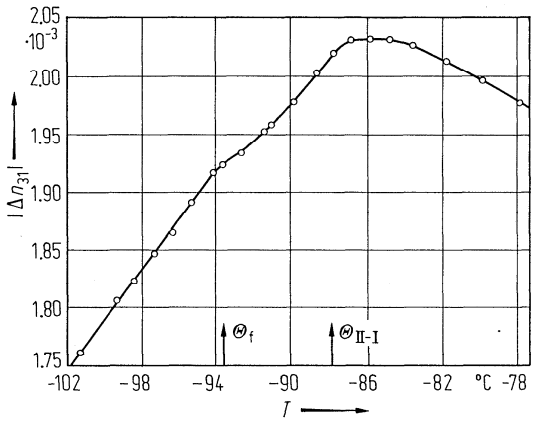

Fig. 39A-3-031. $(NH_4)_2BeF_4$. $|\Delta n_{31}|$ vs. T [76Kon].

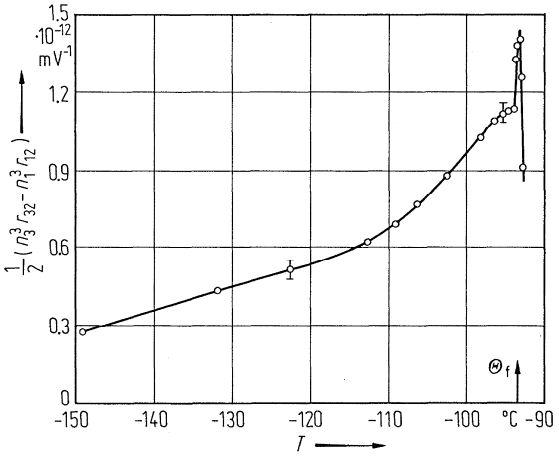

Fig. 39A-3-032. $(NH_4)_2BeF_4$. $\frac{1}{2}\left(n_3^3 r_{32} - n_1^3 r_{12}\right)$ vs. T [76Kon].

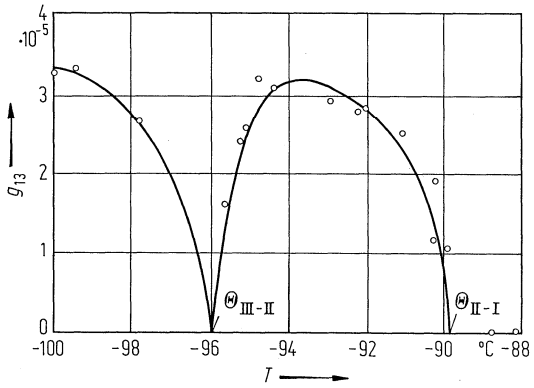

Fig. 39A-3-033. $(NH_4)_2BeF_4$. g_{13} vs. T [85Ues]. g_{13}: gyration tensor component. $\lambda = 632.8$ nm.

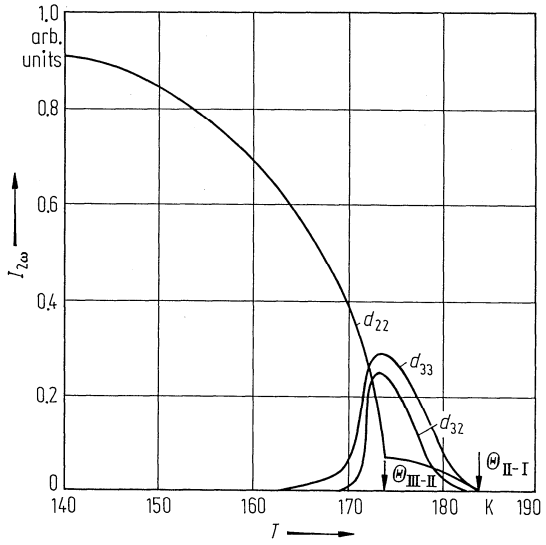

Fig. 39A-3-034. $(NH_4)_2BeF_4$. $I_{2\omega}$ vs. T [79Vty]. $I_{2\omega}$: optical second harmonic intensity.

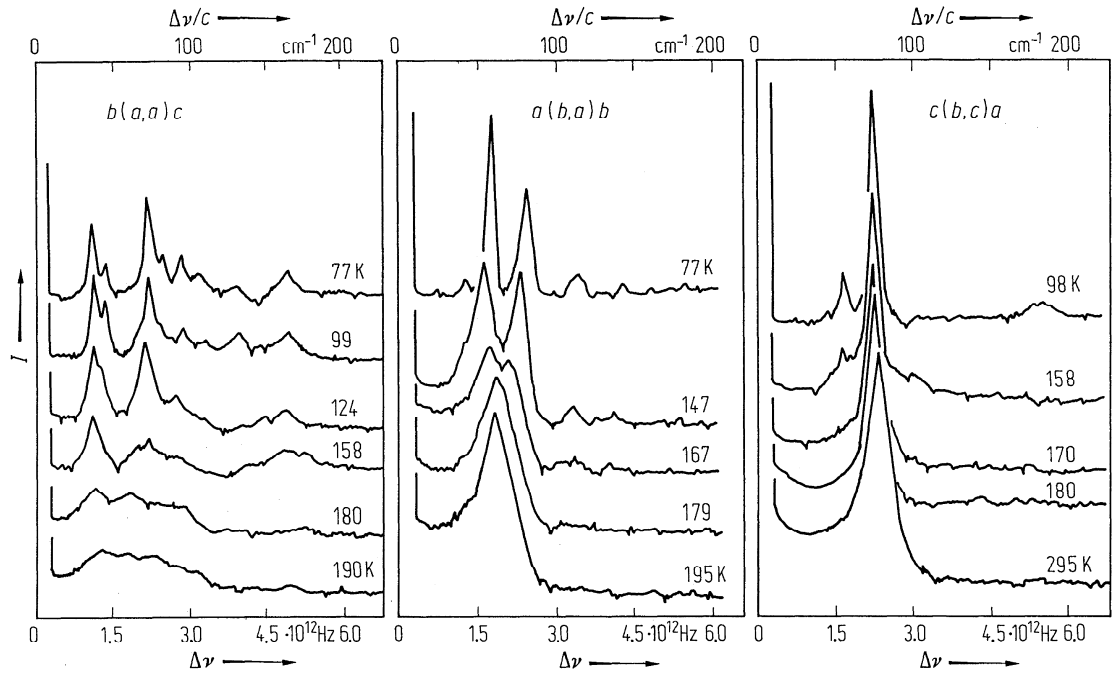

Fig. 39A-3-035. $(NH_4)_2BeF_4$. I vs. $\Delta\nu$ [77Wad]. I: Raman scattering intensity. Parameter: T.

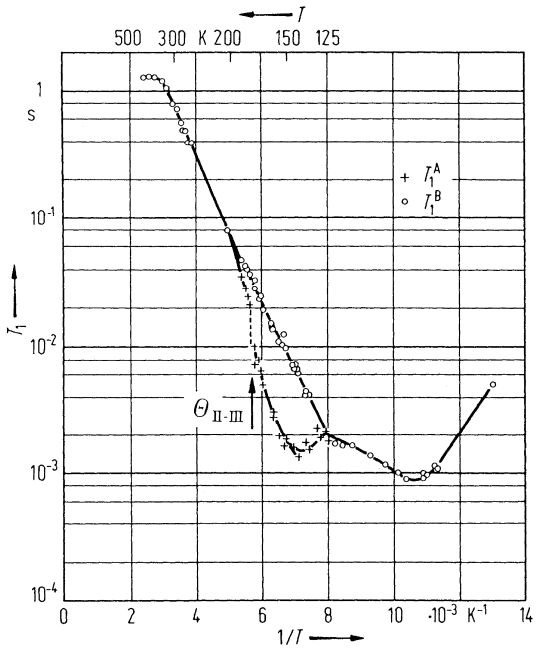

Fig. 39A-3-036. $(ND_4)_2BeF_4$. T_1 vs. $1/T$ [69Kyd]. T_1: deuteron spin-lattice relaxation time. There are two well-separated sets of T_1 around Θ_{III-II}, denoted as T_1^A and T_1^B. ν_L = 11.5 MHz.

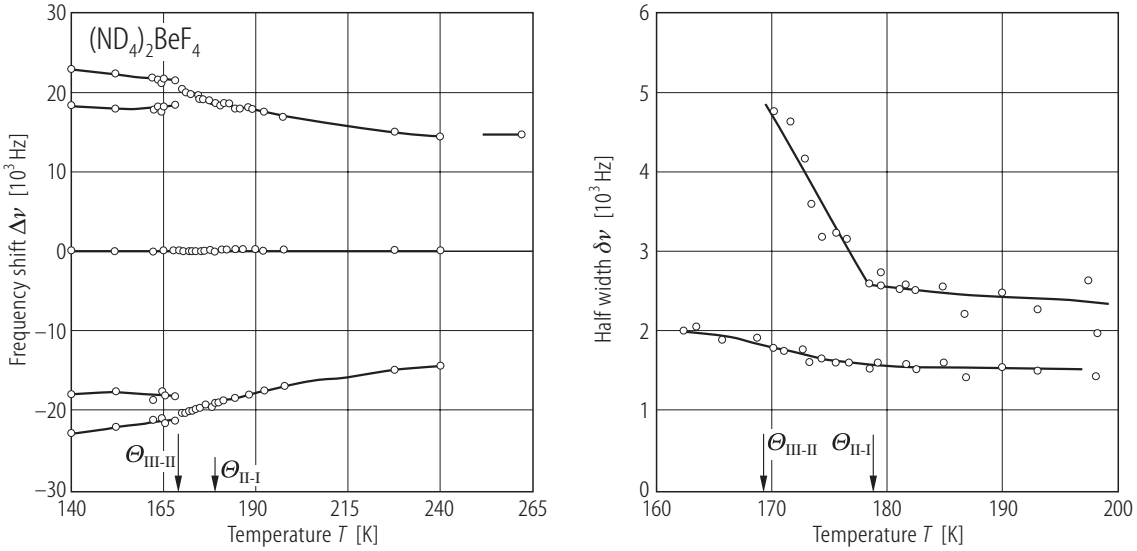

Fig. 39A-3-037. $(ND_4)_2BeF_4$. $\Delta\nu$ vs. T, $\delta\nu$ vs. T [80Rut]. ^{9}Be NMR. ν_L = 37.9 MHz. $\Delta\nu$: frequency shift of satellites from central line. Right figure: half-width of the central line (lower curve) and the satellites (upper curve).

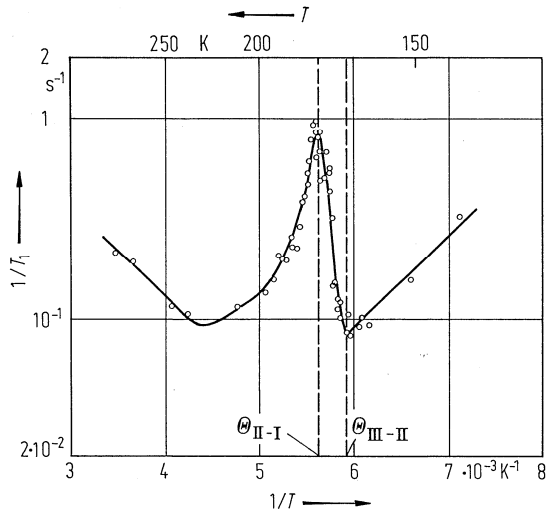

Fig. 39A-3-038. $(ND_4)_2BeF_4$. $1/T_1$ vs. $1/T$ [80Rut]. ^{9}Be spin-lattice relaxation time. ν_L = 37.9 MHz.

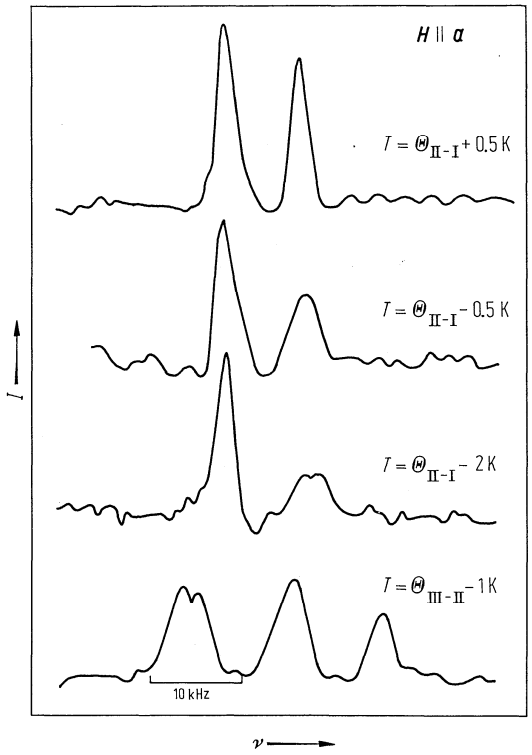

Fig. 39A-3-039. $(NH_4)_2BeF_4$. ^{14}N NMR line shapes [81Bli]. Parameter: T. ν_L = 19.5 MHz.

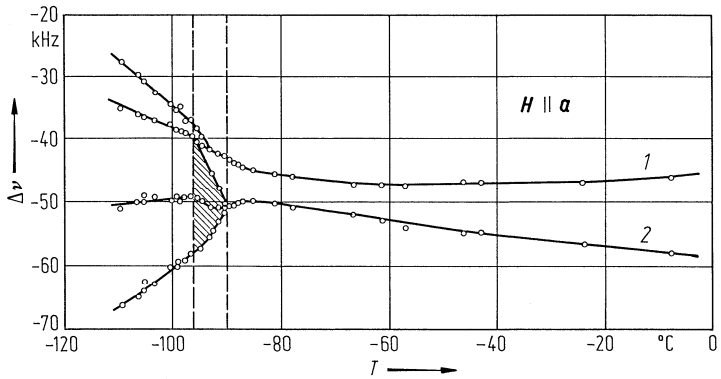

Fig. 39A-3-040. $(NH_4)_2BeF_4$. $\Delta\nu$ vs. T [81Bli]. $\Delta\nu$: ^{14}N quadrupole perturbed frequency shift. ν_L = 19.5 MHz. Hatched area corresponds to broad lines. *1* and *2* correspond to two nonequivalent NH_4 groups.

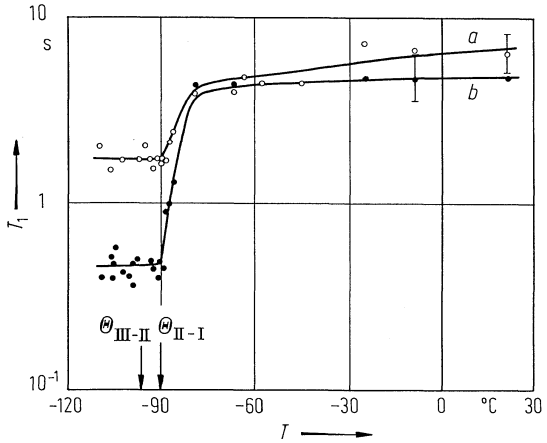

Fig. 39A-3-041. $(NH_4)_2BeF_4$. T_1 vs. T [81Bli]. T_1: ^{14}N spin-lattice relaxation time. ν_L = 19.5 MHz. Curves *a* and *b* correspond to two chemically nonequivalent NH_4 groups.

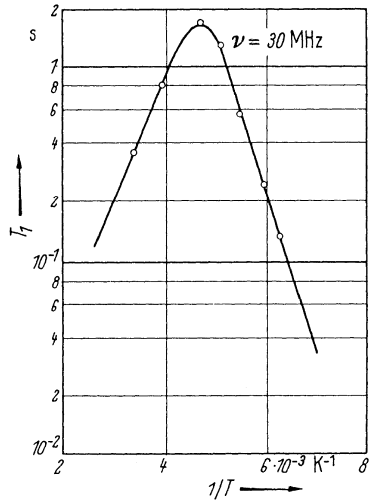

Fig. 39A-3-042. $(NH_4)_2BeF_4$. T_1 vs. $1/T$ [62Mil]. T_1: spin-lattice relaxation time of ^{19}F.

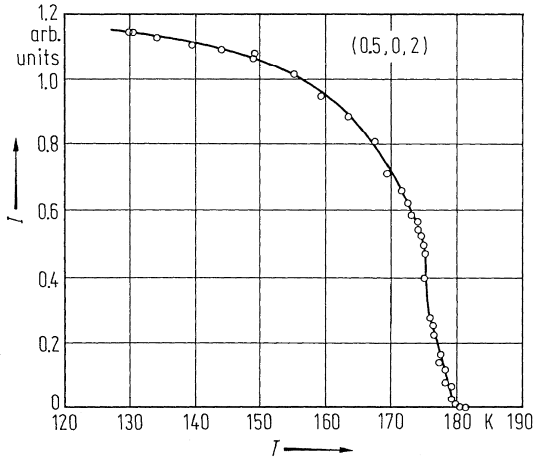

Fig. 39A-3-043. $(NH_4)_2BeF_4$. I vs. T [74Mak]. I: integrated intensity of X-ray superlattice reflection at (1/2, 0, 2).

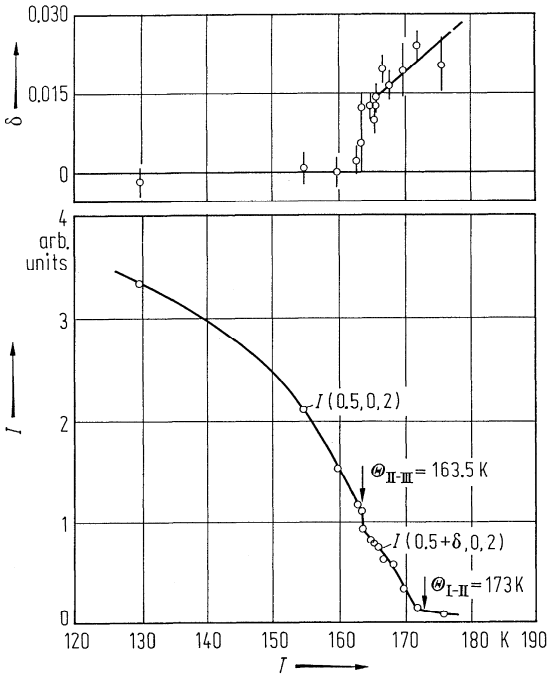

Fig. 39A-3-044. $(ND_4)_2BeF_4$. I, δ vs. T [77Iiz]. I: integrated neutron reflection intensity at $(1/2 + \delta, 0, 2)$. δ: deviation of superlattice position from (1/2, 0, 2).

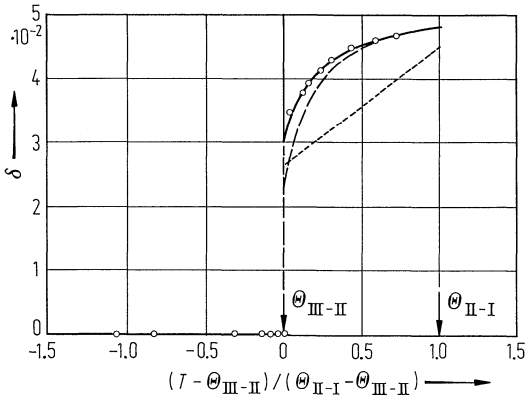

Fig. 39A-3-045. $(NH_4)_2BeF_4$. δ vs. $(T - \Theta_{III-II})/(\Theta_{II-I} - \Theta_{III-II})$ [85Kob]. δ: parameter indicating the position of satellite reflection $((1 + \delta)/2, 0, 2)$ in reciprocal space. Open circles: X-ray scattering [85Kob], long dashed line: X-ray scattering [82Kud], short dashed line: neutron scattering [77Iiz].

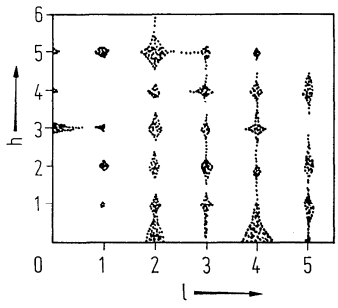

Fig. 39A-3-046. $(NH_4)_2BeF_4$. X-ray diffuse scattering observed in (h, 1/2, l) [77Ono]. T = RT.

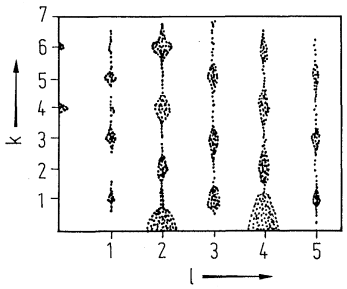

Fig. 39A-3-047. $(NH_4)_2BeF_4$. X-ray diffuse scattering observed in (1/2, k, l) [77Ono]. T = RT.